# Tailoring Photon Statistics with an Atom-Based Two-Photon Interferometer

Martin Cordier,* Max Schemmer,*,† Philipp Schneeweiss, Jürgen Volz, and Arno Rauschenbeutel‡
*Department of Physics, Humboldt-Universität zu Berlin, 10099 Berlin, Germany*

(Received 17 April 2023; accepted 27 September 2023; published 30 October 2023)

Controlling the photon statistics of light is paramount for quantum science and technologies. Recently, we demonstrated that transmitting resonant laser light past an ensemble of two-level emitters can result in a stream of single photons or excess photon pairs. This transformation is due to quantum interference between the transmitted laser light and the incoherently scattered photon pairs [Prasad *et al.*, Nat. Photonics **14**, 719 (2020)]. Here, using the dispersion of the atomic medium, we actively control the relative quantum phase between these two components. We thereby realize a tunable two-photon interferometer and observe interference fringes in the normalized photon coincidence rate. When tuning the relative phase, the coincidence rate varies periodically, giving rise to a continuous modification of the photon statistics from antibunching to bunching. Beyond the fundamental insight that there exists a tunable quantum phase between incoherent and coherent light that dictates the photon statistics, our results lend themselves to the development of novel quantum light sources.

DOI: 10.1103/PhysRevLett.131.183601

Nonclassical light is a resource in science and technology with applications ranging from quantum communication [1] and information processing [2] to sensing [3], imaging [4,5], and metrology [6]. Depending on the respective application, different photon statistics are required, ranging from streams of single photons to photon pairs. While the former are anticorrelated in time and thus exhibit antibunching, an excess of photon pairs manifests itself as time-correlated or bunched detection events. Nonlinear media are an important tool for generating such nonclassical light and are used, e.g., in down-conversion-based quantum light sources [7,8]. The strongest optical nonlinearity is granted by quantum emitters like atoms, molecules, color centers, or quantum dots. Such quantum emitters even allow one to reach the regime of quantum nonlinear optics, where the response of the medium to the incident light strongly differs between one and two incident photons. Because of their intrinsic nonlinear properties, two-level quantum emitters are widely used to generate antibunched light [9–11].

The light scattered by a single emitter is commonly subdivided into two components, namely coherently and incoherently scattered light, reflecting the respective capability to interfere with the field of the excitation laser. About forty years ago, it was conjectured that antibunching in the resonance fluorescence of a two-level emitter stems from destructive quantum interference between scattering a photon pair coherently or incoherently [12,13]. Recently, there has been renewed interest in utilizing this interference phenomenon to generate various quantum states of light [14–16]. Building on this insight, it has been shown that when rejecting one of the components, the photon statistics of the remaining fluorescence light of a single quantum emitter can be modified, from antibunching to Poissonian statistics [17,18] and to bunching [19,20]. Moreover, it has been shown that a similar quantum interference effect occurs when transmitting resonant light past an ensemble of two-level emitters [21,22]. All these demonstrations are limited to modification of the relative power between the coherent and incoherent light, thereby narrowing the range of accessible quantum states.

Here, we demonstrate, for the first time, full control over both the relative phase and amplitude of the coherent and incoherent light that is transmitted through an ensemble of laser-cooled atoms. Taking advantage of the dispersion of the atomic medium, we realize a two-photon interferometer that allows us to continuously tune the nature of the interference from destructive to constructive. Scanning the phase of this interferometer, we observe interference fringes in the photon coincidence rate, thereby supporting the fundamental insight that the quantum phase between the coherent and incoherent light dictates the photon statistics.

Our setup is sketched in Fig. 1(b). It comprises an optical nanofiber through which a continuous wave (CW) laser field is launched with photon flux $|\alpha_{\mathrm{in}}|^2$ and frequency $\omega_{\mathrm{L}}$. In the nanofiber region, the laser light protrudes beyond the nanofiber surface in the form of an evanescent field which couples to an ensemble of $N$ laser-cooled cesium atoms trapped along the nanofiber (D2-line: resonance frequency $\omega_0$, natural linewidth $\Gamma = 2\pi \times 5.2$ MHz [23]). The photon statistics of the transmitted light is measured with a Hanbury-Brown and Twiss setup. Each of the atoms can scatter the incident light coherently and incoherently. In the regime of low saturation, incoherent scattering is a process that resembles spontaneous four-wave mixing where two laser photons are converted into a pair of frequency entangled red- and blue-detuned photons centered around $\omega_L$ [12,24–27],

 

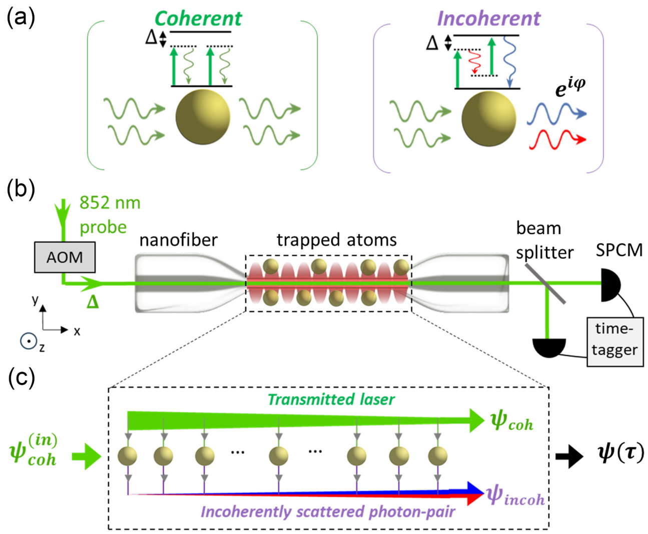


FIG. 1. (a) Illustration of the coherent and incoherent two-photon processes for a single emitter. (b) Experimental setup. Laser-cooled Cs atoms are optically trapped in the evanescent field surrounding an optical nanofiber and interact with a near-resonant CW laser field (green). The detuning between the laser light and the atomic resonance $\Delta$ is set by an acousto-optic modulator (AOM). The transmitted light passes through a 80 MHz bandpass filter that suppresses background light and is wide enough to leave the coherent and incoherent components unaffected [28]. The photon statistic of the transmitted light is measured with two single-photon countermodules in a Hanbury-Brown and Twiss setup. (c) Sketch of the effective multipath interferometer for the coherent (upper arm) and incoherent (lower arm) component of the two-photon wave function. Initially the two-photon component is fully coherent with $\psi_{\mathrm{coh}}^{(\mathrm{in})} = \alpha_{\mathrm{in}}^2/2$. While the coherent and incoherent components are sketched separately, they propagate inside the same spatial mode of the nanofiber.

see Fig. 1(a) right panel. For small laser-atom detuning $|\Delta| < \Gamma$ where $\Delta = \omega_L - \omega_0$, the incoherent component has a width on the order of $\Gamma$ [28]. Notably, this two-photon amplitude interferes with that of the laser light with a relative phase dependent on the laser-atom detuning $\Delta$. More precisely, as the laser light is propagating through an atomic ensemble, one has to add the incoherent scattering amplitudes from each atom. This gives rise to a collective enhancement of the probability amplitude of generating an entangled photon pair [22,26]. At the same time, the incoming laser light is attenuated exponentially with the number of atoms when propagating through the ensemble, according to Beer-Lambert's law. For small atom numbers, the transmitted light is dominated by the laser light, thus resembling an attenuated coherent state. For larger atom numbers, however, the combined effect of exponential attenuation of the laser field and the collective build-up of the incoherent component strongly modifies the state. This manifests itself in a predicted deviation from Beer-Lambert's law in the transmitted power [22,38] as well as a modification of the photon statistics [21,22], owing to the quantum nature of this process. To describe the resulting photon statistic quantitatively, one has to consider the quantum state of the two-photon component of the transmitted light [22]:

$$|\psi\rangle = \iint d\tau_1 d\tau_2 \psi(\tau_2 - \tau_1) \hat{a}_{\tau_1}^\dagger \hat{a}_{\tau_2}^\dagger |0\rangle, \tag{1}$$

where $\hat{a}_{\tau_i}^\dagger$ creates a photon at time $\tau_i$. The temporal wave function $\psi(\tau)$ gives the probability amplitude of detecting two photons with a time delay $\tau = \tau_2 - \tau_1$. In the low saturation regime, this two-photon wave function can be expressed as

$$\psi(\tau) = \psi_{\mathrm{coh}} + \psi_{\mathrm{incoh}}(\tau), \tag{2}$$

where $\psi_{\mathrm{coh}}$ and $\psi_{\mathrm{incoh}}$ are the coherent and incoherent components of the two-photon wave function of the transmitted light, respectively. In order to calculate $\psi_{\mathrm{coh}}$, we apply Beer-Lambert's law to the incident field. The resulting attenuated coherent component consists of uncorrelated photons. Consequently, its two-photon wave function $\psi_{\mathrm{coh}}$ does not depend on $\tau$. In contrast, $\psi_{\mathrm{incoh}}$ describes time-frequency entangled photon pairs whose correlations originate from atom-mediated photon-photon interactions [24]. Correspondingly, this implies that these correlations decay with a time constant given by the excited state lifetime, $\tau_{\mathrm{at}} = 1/\Gamma$. In order to calculate $\psi_{\mathrm{incoh}}$, we sum up the contribution from all atoms. To do so, we first determine, using Beer-Lambert's law, the amplitude of the coherent driving field at the position of each atom. We then compute the incoherent component of the two-photon wave function of the field that is forward-scattered into the waveguide by each atom individually. Finally, we sum up these individual components, taking into account their respective transmission past the downstream atoms. The expression for $\psi_{\mathrm{incoh}}$ as well as its derivation can be found in Sec. S1 of Supplemental Material [28]. We note that $\psi_{\mathrm{incoh}}$ is at the origin of squeezing in the transmitted light and can hence be experimentally deduced from its squeezing spectrum [26].

The resulting second-order quantum correlation function of the transmitted light is proportional to the squared modulus of the two-photon wave function, $g^{(2)}(\tau) \propto |\psi(\tau)|^2$. Thus, $g^{(2)}(\tau)$ can be viewed as the interference signal of the two-photon interferometer sketched in Fig. 1(c). In this picture, each atom acts as a nonlinear beam splitter that splits the incoming light into a coherently and an incoherently scattered component, which are copropagating but can be distinguished by their frequency. At the same time, each atom also imparts a relative phase shift between the coherent and incoherent component. As a consequence, after the interaction with the ensemble, the interfering complex amplitudes, $\psi_{\mathrm{coh}}$ and $\psi_{\mathrm{incoh}}(\tau)$, depend both in magnitude and phase on the laser-atom detuning and the number of atoms. In this context, it is useful to introduce their relative phase $\varphi(\tau) = \arg\{\psi_{\mathrm{incoh}}(\tau)\} - \arg\{\psi_{\mathrm{coh}}\}$ and amplitude $\eta(\tau) = |\psi_{\mathrm{incoh}}(\tau)|/|\psi_{\mathrm{coh}}|$. The relative phase shift depends on the interplay of two effects. First, as depicted in Fig. 1(a), when an entangled photon pair is created by an atom, its relative phase with respect to the local coherent field depends on the laser-atom detuning. Second, because the pair contains frequency components that are red and blue detuned from the laser, they experience different refractive indices than the coherent laser light, resulting in an additional phase shift upon propagation through the remaining ensemble. In the special case of resonant excitation, the red- and blue-detuned photons are generated symmetrically around the atomic resonance, such that the dispersive phase shift accumulated by the photon pair exactly cancels out.

Experimentally, $\varphi(\tau)$ and $\eta(\tau)$ are controlled by adjusting the detuning $\Delta$ with an acousto-optic modulator and the atom number $N$. We control the latter via the loading sequence into the nanofiber-based dipole trap [28]. Figure 2 shows four examples of measured $g^{(2)}(\tau)$ for different values of $\Delta$ and $N$ together with the calculated wave functions $\psi_{\mathrm{coh}}$ and $\psi_{\mathrm{incoh}}(\tau)$ for the same parameters. For each detuning $\Delta$, the atom number was chosen such as to yield equal magnitudes of the coherent and incoherent two-photon amplitude at zero time delay, i.e., $\eta(\tau = 0) = 1$, thereby maximizing the interference visibility. On resonance (first row), both $\psi_{\mathrm{coh}}$ and $\psi_{\mathrm{incoh}}(\tau)$ are real functions.

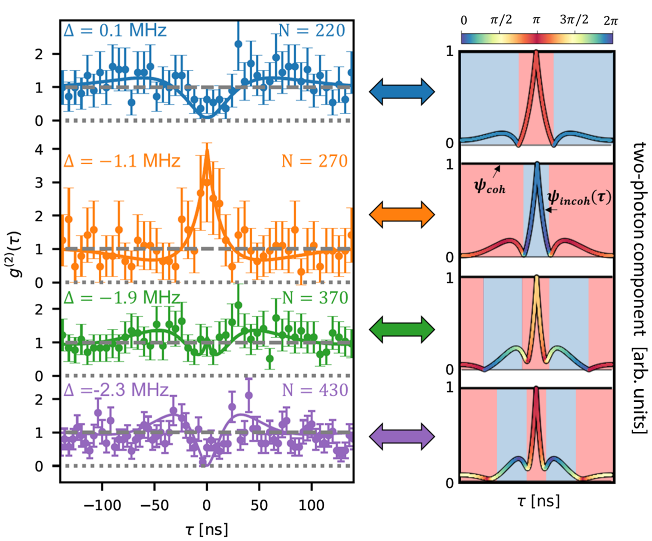


FIG. 2. Left column: measured second-order quantum correlation $g^{(2)}(\tau)$ for different detuning $\Delta$, and thus relative phases $\varphi(\tau = 0)$. The solid lines correspond to the model prediction. In each configuration, the number of atoms is chosen such that we obtain equal amplitudes of the coherent and incoherent two-photon component at zero delay. Right column: corresponding calculated $\psi_{\mathrm{coh}}$ and $\psi_{\mathrm{incoh}}(\tau)$. The color of the line corresponds to the time-dependent phase difference of $\psi_{\mathrm{incoh}}(\tau)$ with respect to $\psi_{\mathrm{coh}}$. The red and blue shaded areas highlight the region where the two components interfere destructively and constructively, respectively.

Around $\tau = 0$, their relative phase is $\varphi(\tau) = \pi$. This leads to destructive interference between the two wave functions, giving rise to photon antibunching in the measured correlation function reaching $g^{(2)}(0) = 0.4 \pm 0.1$ (blue data). For larger delay ($\tau > 45$ ns), $\psi_{\mathrm{incoh}}(\tau)$ changes sign with respect to the coherent component $[\varphi(\tau) = 2\pi]$ and the interference changes from destructive to constructive. In the next three rows, we increase the laser-atom detuning and consequently imprint a phase difference between the coherent and incoherent part, which greatly modifies the interference and, thus, the photon statistics. This is, for instance, illustrated in the second row (orange data) where the detuning was chosen such that, in contrast to the resonant case, $\psi_{\mathrm{coh}}$ and $\psi_{\mathrm{incoh}}$ are in phase and constructively interfere at $\tau = 0$. This results in photon bunching of $g^{(2)}(0) = 2.7 \pm 0.3$, slightly less than $g^{(2)}(0) = 4$, which is the value ideally expected for fully constructive interference and equal amplitudes. Similarly, in the third row (green data), the detuning $\Delta = -1.9$ MHz was chosen to yield a phase shift $\varphi(\tau = 0) = 2\pi/3$ and, accordingly, we measure $g^{(2)}(0) = 1.05 \pm 0.02$, close to the expected value of $g^{(2)}(0) = 1$. At a detuning $\Delta = -2.3$ MHz, as shown in the fourth row (purple data), the two components are again $\pi$ out of phase at zero delay. The remarkable resurrection of antibunching for finite detuning clearly illustrates the interference character of the observed phenomenon. Note that the $\tau$-dependant oscillations in the measured second-order quantum correlation function $g^{(2)}(\tau)$ stem from periodic evolution of the imprinted phase. The frequency of these oscillations increases with the detuning. As a consequence, depending on $\tau$, this leads to either constructive or destructive interferences as indicated by the blue and red shaded area in the right column of Fig. 2.

We now repeat the above measurement procedure for 15 different relative phases $\varphi(\tau = 0)$ and use a maximum likelihood estimation to extract the normalized photon coincidences $g^{(2)}(0)$ [28]. The results of this analysis are plotted in Fig. 3. When modifying the phase difference, the photon statistics oscillates between antibunching and bunching. For comparison, the solid black line shows the theoretical prediction for ideal conditions, $g^{(2)}(0) = 2(1 + \cos[\varphi(0)])$, which oscillates sinusoidally between perfect antibunching for $\varphi(0) = (2n + 1)\pi$ $(n \in \mathbb{Z})$ and photon bunching with $g^{(2)}(0) = 4$ for $\varphi(0) = 2n\pi$. In comparison to this ideal case, our experimental data show a slightly reduced visibility of $V = 0.76 \pm 0.02$. The dashed gray line is a theoretical prediction that includes the effect of averaging over a finite range of atom number that has been used to obtain the data points in Fig. 3. Taking into account this experimental imperfection, the theoretical prediction agrees well with our data.

The observation of interference fringes may come as a surprise given the fact that the two components are spectrally distinguishable, thereby encoding which-way information. However, even under such conditions, interference can be

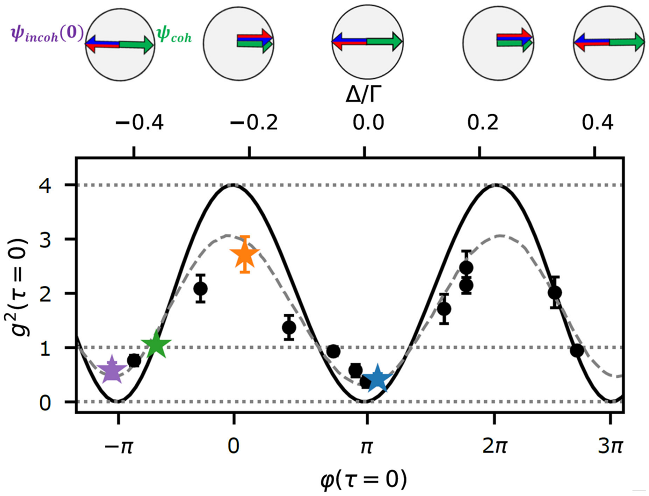


FIG. 3. Interference fringes in the normalized second-order quantum correlation $g^{(2)}(\tau=0)$ as a function of the phase difference between coherent and incoherent photon pairs $\varphi(0)$. All points are measured for equal coherent and incoherent amplitudes at zero delay. The detuning $\Delta$ is shown in the top $x$ axis. The solid line is the model prediction assuming ideal conditions, while the dashed line takes into account the effect of averaging over a finite range of atom numbers [28]. The two arrows in the top column insets represent the complex values of the coherent (green) and the incoherent (blue and red) two-photon amplitude at $\tau=0$. The four data points indicated as stars correspond to the data shown in Fig. 2.

restored by erasing the which-way information [39]. For example, in the double slit experiment [40,41] observing interference requires a detector with a high enough spatial resolution. This consequently erases the which-way information encoded in the transverse momentum of the interfering particle on which slit it passed through. In our experiment, the two paths correspond to a pair of laser photons either being coherently transmitted or incoherently scattered. In this case, the observation of interference in the photon statistics requires a detector with a high enough temporal resolution, which consequently erases the spectral which-way information. We note that a similar effect has been employed when observing the two-photons interference of spectrally distinguishable photons [42].

In conclusion, our results show that the second-order quantum correlation function $g^{(2)}(\tau)$ of near-resonant light transmitted past an ensemble of $N$ two-level emitters can be quantitatively understood as resulting from the interference of the coherent and incoherent components of the two-photon wave function in an atom-based two-photon interferometer. While the two components are typically denominated as coherent and incoherent, the interference fringes observed in our experiment clearly demonstrate that there exists a well-defined phase between both components. This insight and the demonstrated control over their relative amplitude and phase open a new avenue toward tailoring the photon statistics of laser light for application in the realm of quantum technologies or quantum metrology.

In that context, while the current study focuses on the interference of the two-photon component, the same interference mechanism will occur for larger photon-number components, allowing one to engineer higher order correlation functions. This may then pave the way for the generation of complex quantum states of light with larger photon number and tailored temporal correlations.

We are grateful to J. Dalibard for his feedback and careful reading of the manuscript. M. C. and M. S. acknowledge support from the European Commission (Marie Skłodowska-Curie Individual Fellowship Grants No. 101029304 and No. 896957). We acknowledge funding by the Alexander von Humboldt Foundation in the framework of the Alexander von Humboldt Professorship endowed by the Federal Ministry of Education and Research, as well as funding by the European Commission under the project DAALI (No. 899275).

*These authors contributed equally to this work.
†Present address: Istituto Nazionale di Ottica, Consiglio Nazionale delle Ricerche, 50019 Sesto Fiorentino, Italy.
‡arno.rauschenbeutel@hu-berlin.de

[1] J. Yin *et al.*, Science **356**, 1140 (2017).
[2] H.-S. Zhong *et al.*, Science **370**, 1460 (2020).
[3] M. W. Mitchell, J. S. Lundeen, and A. M. Steinberg, Nature (London) **429**, 161 (2004).
[4] D. Gatto Monticone, K. Katamadze, P. Traina, E. Moreva, J. Forneris, I. Ruo-Berchera, P. Olivero, I. P. Degiovanni, G. Brida, and M. Genovese, Phys. Rev. Lett. **113**, 143602 (2014).
[5] I. Kviatkovsky, H. M. Chrzanowski, E. G. Avery, H. Bartolomaeus, and S. Ramelow, Sci. Adv. **6**, abd0264 (2020).
[6] J. Aasi *et al.*, Nat. Photonics **7**, 613 (2013).
[7] J. Wang, S. Paesani, Y. Ding, R. Santagati, P. Skrzypczyk, A. Salavrakos, J. Tura, R. Augusiak, L. Mančinska, D. Bacco, D. Bonneau, J. W. Silverstone, Q. Gong, A. Acín, K. Rottwitt, L. K. Oxenløwe, J. L. O'Brien, A. Laing, and M. G. Thompson, Science **360**, 285 (2018).
[8] H.-S. Zhong, Y. Li, W. Li, L.-C. Peng, Z.-E. Su, Y. Hu, Y.-M. He, X. Ding, W. Zhang, H. Li, L. Zhang, Z. Wang, L. You, X.-L. Wang, X. Jiang, L. Li, Y.-A. Chen, N.-L. Liu, C.-Y. Lu, and J.-W. Pan, Phys. Rev. Lett. **121**, 250505 (2018).
[9] P. Senellart, G. Solomon, and A. White, Nat. Nanotechnol. **12**, 1026 (2017).
[10] F. Lenzini, N. Gruhler, N. Walter, and W. H. P. Pernice, Adv. Quantum Technol. **1**, 1800061 (2018).
[11] M. Rezai, J. Wrachtrup, and I. Gerhardt, Phys. Rev. X **8**, 031026 (2018).
[12] J. Dalibard and S. Reynaud, J. Phys. **44**, 1337 (1983).
[13] A. Aspect, G. Roger, S. Reynaud, J. Dalibard, and C. Cohen-Tannoudji, Phys. Rev. Lett. **45**, 617 (1980).

[14] E. del Valle, A. Gonzalez-Tudela, F. P. Laussy, C. Tejedor, and M. J. Hartmann, Phys. Rev. Lett. **109**, 183601 (2012).
[15] J. C. López Carreño, E. Z. Casalengua, F. P. Laussy, and E. del Valle, Quantum Sci. Technol. **3**, 045001 (2018).
[16] E. Z. Casalengua, J. C. L. Carreño, F. P. Laussy, and E. del Valle, Phys. Rev. A **101**, 063824 (2020).
[17] L. Hanschke, L. Schweickert, J. C. L. Carreño, E. Schöll, K. D. Zeuner, T. Lettner, E. Z. Casalengua, M. Reindl, S. F. C. da Silva, R. Trotta, J. J. Finley, A. Rastelli, E. del Valle, F. P. Laussy, V. Zwiller, K. Müller, and K. D. Jöns, Phys. Rev. Lett. **125**, 170402 (2020).
[18] C. L. Phillips, A. J. Brash, D. P. S. McCutcheon, J. Iles-Smith, E. Clarke, B. Royall, M. S. Skolnick, A. M. Fox, and A. Nazir, Phys. Rev. Lett. **125**, 043603 (2020).
[19] A. Ulhaq, S. Weiler, S. M. Ulrich, R. Roßbach, M. Jetter, and P. Michler, Nat. Photonics **6**, 238 (2012).
[20] L. Masters, X.-X. Hu, M. Cordier, G. Maron, L. Pache, A. Rauschenbeutel, M. Schemmer, and J. Volz, Nat. Photonics (2023).
[21] A. S. Prasad, J. Hinney, S. Mahmoodian, K. Hammerer, S. Rind, P. Schneeweiss, A. S. Sørensen, J. Volz, and A. Rauschenbeutel, Nat. Photonics **14**, 719 (2020).
[22] S. Mahmoodian, M. Čepulkovskis, S. Das, P. Lodahl, K. Hammerer, and A. S. Sørensen, Phys. Rev. Lett. **121**, 143601 (2018).
[23] R. J. Rafac, C. E. Tanner, A. E. Livingston, and H. G. Berry, Phys. Rev. A **60**, 3648 (1999).
[24] J.-T. Shen and S. Fan, Phys. Rev. A **76**, 062709 (2007).
[25] H. Le Jeannic, T. Ramos, S. F. Simonsen, T. Pregnolato, Z. Liu, R. Schott, A. D. Wieck, A. Ludwig, N. Rotenberg, J. J. García-Ripoll, and P. Lodahl, Phys. Rev. Lett. **126**, 023603 (2021).
[26] J. Hinney, A. S. Prasad, S. Mahmoodian, K. Hammerer, A. Rauschenbeutel, P. Schneeweiss, J. Volz, and M. Schemmer, Phys. Rev. Lett. **127**, 123602 (2021).
[27] B. L. Ng, C. H. Chow, and C. Kurtsiefer, Phys. Rev. A **106**, 063719 (2022).
[28] See Supplemental Material at http://link.aps.org/supplemental/10.1103/PhysRevLett.131.183601 which includes Refs. [29–37], for more details on the theoretical model, the experimental parameters and methods. as well as on the analysis of the data.
[29] D. Reitz, C. Sayrin, B. Albrecht, I. Mazets, R. Mitsch, P. Schneeweiss, and A. Rauschenbeutel, Phys. Rev. A **89**, 031804(R) (2014).
[30] R. Mitsch, C. Sayrin, B. Albrecht, P. Schneeweiss, and A. Rauschenbeutel, Nat. Commun. **5**, 5713 (2014).
[31] K. J. Kusmierek, S. Mahmoodian, M. Cordier, J. Hinney, A. Rauschenbeutel, M. Schemmer, P. Schneeweiss, J. Volz, and K. Hammerer, SciPost Phys. Core **6**, 041 (2023).
[32] F. Le Kien, V. I. Balykin, and K. Hakuta, Phys. Rev. A **70**, 063403 (2004).
[33] A. Goban, K. S. Choi, D. J. Alton, D. Ding, C. Lacroûte, M. Pototschnig, T. Thiele, N. P. Stern, and H. J. Kimble, Phys. Rev. Lett. **109**, 033603 (2012).
[34] E. Vetsch, D. Reitz, G. Sagué, R. Schmidt, S. T. Dawkins, and A. Rauschenbeutel, Phys. Rev. Lett. **104**, 203603 (2010).
[35] N. V. Corzo, B. Gouraud, A. Chandra, A. Goban, A. S. Sheremet, D. V. Kupriyanov, and J. Laurat, Phys. Rev. Lett. **117**, 133603 (2016).
[36] N. Schlosser, G. Reymond, and P. Grangier, Phys. Rev. Lett. **89**, 023005 (2002).
[37] H. Abitan, H. Bohr, and P. Buchhave, Appl. Opt. **47**, 5354 (2008).
[38] R. Veyron, V. Mancois, J.-B. Gerent, G. Baclet, P. Bouyer, and S. Bernon, Phys. Rev. Res. **4**, 033033 (2022).
[39] J. A. Wheeler and W. H. Zurek, *Quantum Theory and Measurement* (Princeton University Press, Princeton, NJ, 2014).
[40] O. Carnal and J. Mlynek, Phys. Rev. Lett. **66**, 2689 (1991).
[41] S. P. Walborn, M. O. Terra Cunha, S. Pádua, and C. H. Monken, Phys. Rev. A **65**, 033818 (2002).
[42] T. Legero, T. Wilk, M. Hennrich, G. Rempe, and A. Kuhn, Phys. Rev. Lett. **93**, 070503 (2004).